Article

Current Biology

Optogenetic Rescue of a Patterning Mutant

Graphical Abstract

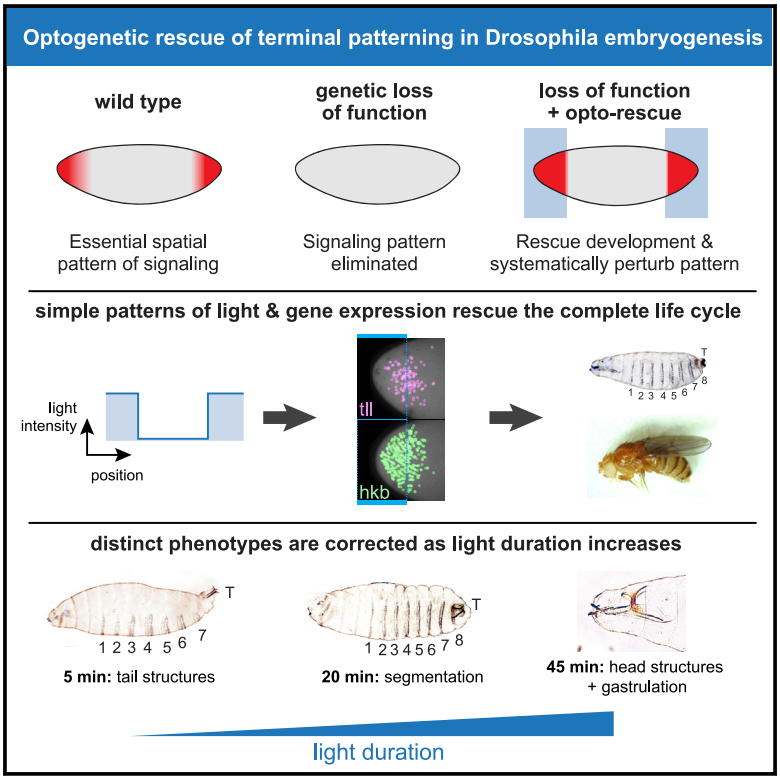

Highlights

- Local optogenetic stimulation rescues the lethal loss of a developmental pattern
- Opto-rescued embryos hatch, reach adulthood, mate, and lay eggs normally
- Simple light inputs can still rescue despite lacking graded information
- Distinct phenotypes are rescued at increasing light thresholds in a switch-like manner

Authors

Heath E. Johnson, Nareg J.V. Djabrayan, Stanislav Y. Shvartsman, Jared E. Toettcher

Correspondence

toettcher@princeton.edu

In Brief

Johnson et al. show that the genetic loss of a developmental pattern—terminal signaling in the Drosophila embryo—can be rescued by optogenetic stimulation of Ras. Such optical control over development could be used to probe cell- and tissue-level regulation, engineer tissue organization, and correct developmental defects.

Johnson et al., 2020, Current Biology *30*, 3414–3424
September 7, 2020
https://doi.org/10.1016/j.cub.2020.06.059

CellPress

CellPress

Current Biology

Article

Optogenetic Rescue of a Patterning Mutant

Heath E. Johnson,[1] Nareg J.V. Djabrayan,[2] Stanislav Y. Shvartsman,[2,3,4] and Jared E. Toettcher[1,5,*]
[1]Department of Molecular Biology, Princeton University, Princeton, NJ 08544, USA
[2]Department of Chemical and Biological Engineering, Princeton University, Princeton, NJ 08544, USA
[3]Lewis Sigler Institute for Integrative Genomics, Princeton University, Princeton, NJ 08544, USA
[4]Center for Computational Biology, Flatiron Institute, New York, NY 10010, USA
[5]Lead Contact
*Correspondence: toettcher@princeton.edu
https://doi.org/10.1016/j.cub.2020.06.059

SUMMARY

Animal embryos are patterned by a handful of highly conserved inductive signals. Yet, in most cases, it is unknown which pattern features (i.e., spatial gradients or temporal dynamics) are required to support normal development. An ideal experiment to address this question would be to "paint" arbitrary synthetic signaling patterns on "blank canvas" embryos to dissect their requirements. Here, we demonstrate exactly this capability by combining optogenetic control of Ras/extracellular signal-related kinase (ERK) signaling with the genetic loss of the receptor tyrosine-kinase-driven terminal signaling patterning in early *Drosophila* embryos. Blue-light illumination at the embryonic termini for 90 min was sufficient to rescue normal development, generating viable larvae and fertile adults from an otherwise lethal terminal signaling mutant. Optogenetic rescue was possible even using a simple, all-or-none light input that reduced the gradient of Erk activity and eliminated spatiotemporal differences in terminal gap gene expression. Systematically varying illumination parameters further revealed that at least three distinct developmental programs are triggered at different signaling thresholds and that the morphogenetic movements of gastrulation are robust to a 3-fold variation in the posterior pattern width. These results open the door to controlling tissue organization with simple optical stimuli, providing new tools to probe natural developmental processes, create synthetic tissues with defined organization, or directly correct the patterning errors that underlie developmental defects.

INTRODUCTION

During animal development, the embryo is patterned by gradients of protein activity that define cells' positions along the body axes and within developing tissues [1]. In recent years, many developmental patterns have been characterized in precise quantitative detail in individual embryos [2–4]. Yet in nearly every case, it remains unknown which features of signaling patterns carry essential information: the instantaneous protein concentration; the area under the curve; or the total duration of signaling above a threshold. The quantity of information contained in a single pattern also remains mysterious: how many distinct levels are read out by the genetic networks that serve as signal interpretation systems and how long does it take to transfer this information?

To address these questions, we envisioned an idealized experiment to better define the information contained in a developmental pattern (Figure 1A) [5]. First, one might prepare mutant embryos in which a specific signaling pattern is completely eliminated. On this background, one might then apply a synthetic signaling pattern, varying features such as its shape, intensity, or duration and monitoring the capability of each to rescue the developmental process. Although such an experiment has historically been intractable, we reasoned optogenetic control over cell signaling opens the door to exactly this capability. An appropriately tailored light input could be used to produce any spatiotemporal signaling pattern, enabling a biologist to test for the minimal features required to support proper development or allowing a bioengineer to apply non-natural stimuli to implement novel tissue architectures or morphogenetic programs [5–7].

We thus set out to perform an optogenetic rescue of terminal signaling, the first pattern of receptor tyrosine kinase (RTK) activity during *Drosophila* embryogenesis [8]. Terminal signaling is orchestrated by localized activation of the RTK Torso (Tor) by its ligand Trunk (Trk) at the embryonic anterior and posterior poles (Figure 1B). Quantitative studies of terminal signaling in individual embryos have revealed a reproducible terminal-to-interior gradient that is dynamically established over a 2-h window in early embryogenesis [9]. This gradient is essential: embryos from mothers lacking Tor, Trk, or the required co-factor Torso-like (Tsl) completely lack a terminal signaling gradient and are defective in a wide variety of anterior- and posterior-localized processes, including the formation of mouth parts and tail structures, the differentiation of many endoderm-derived tissues, and the ability to coordinate tissue movements during gastrulation [10, 11]. Yet the nature and quantity of information contained in the terminal pattern are still unclear. The naturally observed

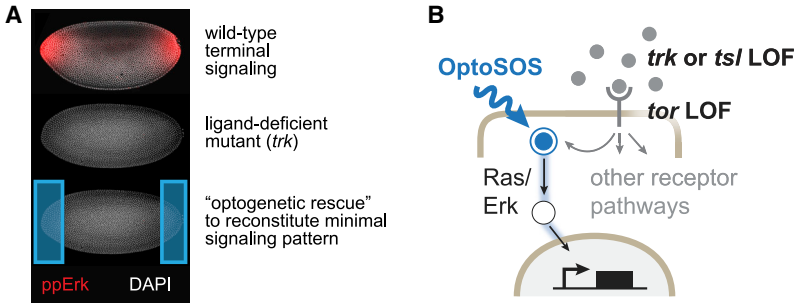

Figure 1. Painting Developmental Signaling Patterns on a Blank Canvas

(A) Upper: immunofluorescence (IF) for doubly phosphorylated extracellular signal-related kinase (Erk) (ppErk; red) in a nuclear cycle 14 (NC14) embryo, exhibiting the characteristic terminal gradient. Middle: IF for ppErk in a *trk*^{1} mutant NC14 embryo shows complete loss of terminal ppErk at the termini. Lower: schematic of the proposed experiment is shown, where light is applied on the *trk* mutant background to potentially restore Erk activity and function. All embryos in the figure are oriented with anterior to the left and ventral downward.

(B) Because the light-activated OptoSOS system directly activates Ras/Erk pathway downstream of receptor tyrosine kinases, it can be functionally combined with the genetic loss of Tor, Tsl or Trk, the three receptor-level components normally active at the embryonic termini.

See also Figure S1.

gradient of Tor activity leads to expression of the two classic terminal gap genes Tll and Hkb in distinct but overlapping domains, supporting the notion that spatiotemporal variations in pathway activity play an important role [12–14]. On the other hand, seminal prior work demonstrated that many features of the terminal loss-of-function phenotype could be rescued by supplying rather crude sources of activity, for example, by injection of *tor* RNA or constitutively active Ras protein at the poles [15, 16]. The precise requirements for a rescuing terminal pattern thus remain to be defined.

Here, we report rescue of the full *Drosophila* life cycle from OptoSOS-*trk* embryos that completely lack receptor-level terminal signaling but whose Ras/Erk signaling can be controlled with light. Illuminated OptoSOS-*trk* embryos develop normal head and tail structures, gastrulate normally, hatch, metamorphose, mate, and lay eggs. Full phenotypic rescue is possible despite the use of simple all-or-none light inputs that limit the graded information contained in the terminal pattern, for example, eliminating expression differences in reporters of the terminal gap genes *tll* and *hkb*. We define the lower essential limits of terminal signaling, demonstrating that at least three distinct developmental switches are triggered at successively increasing illumination thresholds. Our study thus demonstrates that Ras activation by Son of Sevenless (SOS) is sufficient to recapitulate all the essential features of receptor tyrosine kinase signaling at the embryonic termini. It also suggests the spatial gradients of Erk activity normally observed at the termini are not required, at least in the presence of the embryo's additional sources of anterior-posterior positional information. These data provide a first step toward defining the essential information contained in developmental signaling patterns and open the door to optically programming cell fates and tissue movements with high precision in developing tissues.

RESULTS

Light-Controlled Terminal Signaling Rescues Normal Development

We first set out to establish a genetic background where light could be used as the sole source of Erk activity at the embryonic termini, so that its ability to rescue subsequent development could be assessed. Two attributes make terminal signaling an ideal system for optogenetic rescue. First, all three components of the Trk-Tor-Tsl receptor/ligand system are maternal-effect genes [10], so flies that are homozygous null for any of the three genes develop normally, provided that the gene products are maternally deposited in the egg to produce the terminal pattern. Thus, in principle, one may be able to rescue the organism's full life cycle by replacing this single developmental pattern with light. Second, we previously developed the OptoSOS optogenetic system for control over Ras/Erk signaling, a key downstream effector pathway of terminal signaling, in contexts ranging from cultured mammalian cells [17, 18] to the *Drosophila* embryo [19, 20]. In this system, a switch from darkness to light induces SOS membrane localization within seconds, followed by Erk activation and expression of Erk-dependent target genes (e.g., *tll* in the case of the early *Drosophila* embryo; see [19]), whereas a switch to darkness triggers a rapid reversal of this process, returning Erk activity and gene expression to their baselines also on a timescale of minutes [17, 21, 22]. OptoSOS is ideal for attempting light-based rescue because it activates Ras downstream of receptor-level stimulation (Figure 1B) and can thus be combined with mutations targeting receptor-level signaling to place terminal Ras/Erk signaling solely under optogenetic control [23]. Indeed, in preliminary experiments comparing embryos harboring loss-of-function perturbations targeting receptor/ligand signaling (*trk* and *tsl* loss-of-function mutants and a Tor RNAi line; Figures S1 and 1A), we found that OptoSOS-expressing embryos produced from *trk*^{1} mothers lack all endogenous terminal signaling activity [24], but when placed under uniform blue light, these embryos exhibit phenotypes associated with strong gain-of-function terminal signaling [19]. We thus focused on these "OptoSOS-*trk*" embryos for subsequent experiments.

We next set out to determine whether applying light to OptoSOS-*trk* embryos would be sufficient to restore various embryonic structures that are dependent on terminal signaling and, if so, which features of the stimulus might prove to be essential. We began with a simple light stimulus: binary, all-or-none illumination of the anterior or posterior pole. We matched the light stimulus duration (90 min), spatial range (roughly 15% of the embryo's length), and intensity level (one pulse every 30 s) to roughly match the parameters observed for doubly phosphorylated Erk during endogenous terminal signaling, which we quantified here (Figure S2) and in a prior study [4]. Such an optogenetic stimulus should eliminate both the complex temporal

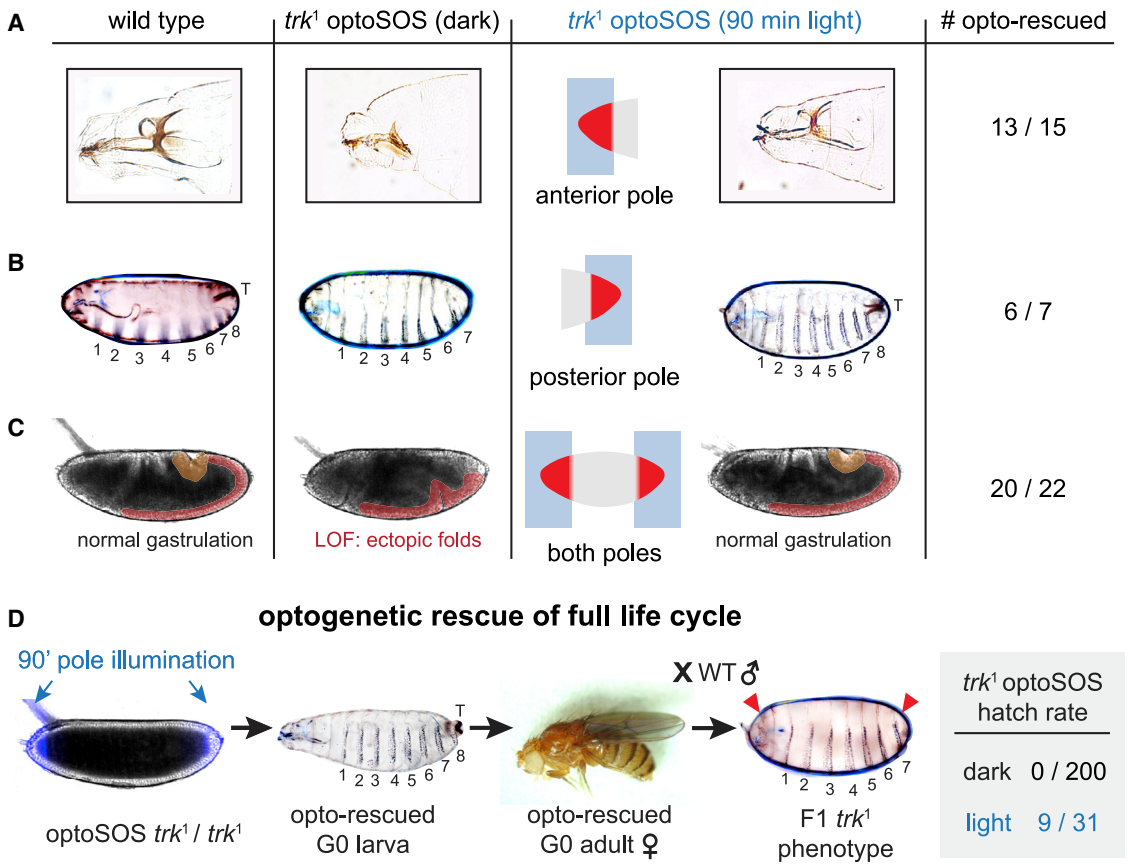

Figure 2. Light-Controlled Terminal Signaling Rescues Normal Development

(A and B) Cuticle preparations from embryos that were illuminated for 90 min at the anterior-most 15% of the embryo (in A) or posterior-most 15% of the embryo (in B) with 0.6-s pulses of saturating blue light delivered every 30 s. Head structures, the 8th abdominal segment, and tail structures (marked "T") are formed normally in wild-type embryos (left images) and are truncated or absent in embryos lacking terminal signaling (middle images) but are rescued after 90 min of illumination at the appropriate pole (right images).

(C) Still images from DIC time-lapse videos of gastrulation in wild-type embryos, OptoSOS-*trk* embryos without illumination, and OptoSOS-*trk* embryos illuminated at both poles. Highlighted regions mark posterior midgut invagination (yellow) and germband elongation (red).

(D) Complete rescue of OptoSOS-*trk* animal development by 90 min illumination at both the anterior-most and posterior-most 15% of the embryo with 0.6-s pulses of saturating blue light delivered every 30 s. Embryos hatch, eclose, and mate. The embryos produced by female light-rescued flies exhibit the *trk* mutant phenotype (red arrows). All embryos in the figure are oriented with anterior to the left and ventral downward.

See also Figure S2, Tables S1 and S2, and Video S1.

dynamics and spatial gradient of the endogenous terminal pattern. Yet even this simple all-or-none light stimulus, delivered to the anterior pole, was sufficient to restore head structures that were indistinguishable from those in wild-type embryos (Figure 2A; see Table S1 for number of embryos with rescued phenotypes). Similar results were obtained upon posterior illumination, which was sufficient to restore the formation of tail structures, such as posterior spiracles, as well as the 8th abdominal segment (Figure 2B).

To assess the rescue of other terminal signaling-dependent processes that are difficult to individually monitor, we applied similar all-or-none light patterns at both embryonic termini and visualized the remainder of their development by differential interference contrast (DIC) microscopy (Figure 2C). Approximately 30% of the embryos illuminated in this manner were able to gastrulate normally, complete the remainder of embryogenesis, and hatch from the imaging device (Video S1). We collected larvae that hatched on the microscope and maintained them in standard tubes, where they proceeded normally through each instar, pupated, and produced normal adult flies (Figure 2D). Finally, we reasoned that optogenetically rescued female adult flies produced in this manner should still be *trk* null, so the embryos produced by these females should still harbor phenotypes consistent with the maternal loss of terminal signaling. Indeed, all embryos laid from light-rescued mothers failed to hatch, and cuticle preparations revealed the *trk* phenotype in all progeny (head defects; absence of the 8th abdominal segment and tail structures; Figure 2D). Taken together, these data confirm the optogenetic rescue of terminal signaling in *Drosophila* embryogenesis. Simple synthetic signaling patterns, generated by local blue light illumination, were thus sufficient to overcome lethal defects in body segmentation, tissue morphogenesis, and cell differentiation to restore the entirety of the fly's life cycle.

Optogenetic Stimulation Eliminates Differences in Terminal Gap Gene Expression Domains

Our optogenetic stimulation experiments relied on all-or-none light inputs, stimuli which we previously found to result in precise, subcellular spatial control over SOS membrane recruitment in the early *Drosophila* embryo [20]. However, many processes may still act to blur these precise inputs into a spatially graded response (e.g., light scattering, diffusion of active components of the Ras/mitogen-activated protein kinase [MAPK] pathway within the syncytial embryo, or other gradients of gene expression along the anterior-posterior axis that might modulate the activity of the terminal signaling pathway). We thus set out to quantify the spatial distribution of Erk activity and downstream gene expression in response to the same all-or-none light stimulus used in our optogenetic rescue experiments. To circumvent the challenge of fixing and staining individual locally illuminated embryos, we relied on live-cell fluorescent biosensors to measure Erk activity and gene expression with high spatiotemporal resolution.

To measure Erk activity, we turned to a recently developed biosensor, miniCic, that translocates from the nucleus to cytosol upon phosphorylation by Erk in *Drosophila* (Figure S3A) [25]. We generated embryos that co-expressed miniCic-mCherry and the OptoSOS system (STAR Methods) and verified that this system could indeed be used in the early embryo by visualizing the endogenous terminal signaling gradient (Figure S3B). We then locally illuminated embryos and quantified nuclear miniCic as a function of position from the edge of our illumination pattern (Figures S3C–S3F). As a control, we quantified nuclear miniCic from the embryo's poles along the endogenous terminal gradient. We fitted Hill curves to each embryo's nuclear miniCic intensity as a function of position to measure the distance over which Erk was active as well as the steepness of its on-to-off switch (Figures S3G and S3H). We found that light could be used to trigger patterns on a shorter length scale than the endogenous gradient: miniCic localization returned to baseline within 60 μm from the edge of the illuminated region versus extending 120 μm from the termini in the endogenous pattern (Figure S3G). Light also resulted in a steeper on-to-off switch, measured by the distance over which miniCic localization switched from 10% to 90% of its baseline nuclear intensity (Figure S3H). Our approach likely over-estimates the sharpness of the endogenous pattern, as kinase biosensors are typically quite sensitive and can become saturated at sub-maximal levels of pathway activity [26], leading a shallow, high-amplitude gradient of Erk activity [4] to be clipped at the biosensor's maximum value and thus appear to switch over a shorter range than the true activity gradient.

We next set out to characterize the spatial patterns of two Erk-dependent target genes, *tll* and *hkb*, that act to specify terminal cell fates and which are normally expressed in distinct domains. Prior studies revealed that *tll* is normally expressed over a broader range than *hkb* [20, 27, 28], a finding that is consistent with activation of *tll* by lower levels of active Erk [13, 19]. We generated embryos that expressed a fluorescent MS2 coat protein (MCP) and where either the *tll* and *hkb* upstream regulatory sequences drove expression of MS2-tagged mRNAs, in genetic backgrounds with normal terminal patterning or a variant of our optogenetic rescue system (OptoSOS-*tsl*; STAR Methods; Figure 3A; Video S2) [21]. Imaging the endogenous terminal pattern revealed distinct domains of *tll* and *hkb* transcriptional foci as expected, with *tll* expressed earlier (nuclear cycle 11 [NC11] to early NC14) and over a broader domain and *hkb* expressed primarily during NC13 to NC14 and localized more tightly at the poles (Figure 3A, right panels; see Figure S3I for quantification over time). These distributions of RNA production were in good agreement with previously measured distributions of total *tll* and *hkb* RNA [20].

In contrast, stimulating OptoSOS-*tsl* embryos under the same all-or-none illumination conditions previously used for optogenetic rescue (0.6-s pulses every 30 s to the anterior-most and posterior-most 15% of individual embryos) produced a different result (Figure 3B). In this case, the expression domains for *tll* and *hkb* more closely matched one another in induction timing and spatial range. Both reporters exhibited transcriptional bursts in response to light that appeared between NC10 and NC13, increasing in NC14 until gastrulation (Figures 3B and S3J). The spatial distribution of gene expression was also similar across both reporters and resembled the broad distribution of the endogenous *tll* pattern (Figure 3C). We quantified the boundary of gene expression from the posterior pole in multiple light-stimulated embryos, which confirmed our observations and also revealed that terminal gene expression extended some tens of micrometers beyond the edge of the illumination pattern, just as had been observed for miniCic nuclear export (Figure 3D). No terminal gap gene expression was observed in control, dark-incubated OptoSOS-*tsl* embryos (Figures S3K and S3L).

Taken together, our data indicate that our all-or-none "rescue stimulus" also substantially reduces the amount of graded information contained within the terminal pattern. Most crucially, it eliminates major differences in the spatial domains and timing for reporters of *tll* and *hkb*, two target genes thought to mediate the majority, if not the entirety, of the embryo's response to terminal signaling. Although some caution must be used in interpreting transcriptional reporters of regulatory regions, these reporters match the endogenous domains of *tll* and *hkb* expression and are activated only in response to OptoSOS stimulation, suggesting that at least Erk-dependent responses are intact and accurate. Importantly, quantification of Erk activity and transcriptional responses revealed that even our sharp, localized light stimulus is blurred tens of micrometers in the context of the embryo, suggesting that graded information is reduced, but not perfectly eliminated, by our optogenetic stimulus. Because the patterns of Erk activity and gene expression extend substantially further from the edge of the illumination pattern than the sharp boundaries of SOScat membrane recruitment [20], they likely do not represent light scattering but rather reflect downstream intracellular processes, such as signal propagation through the cytosolic MAP kinase cascade [29] or cytosolic flow during syncytial nuclear division cycles [30].

At Least Three Levels of Terminal Signaling Trigger Distinct Developmental Programs

The rescue of all anterior and posterior tissue responses by a single all-or-none light pattern is consistent with two different models of terminal cell fate choice. First, Erk activity may be sensed by a single downstream program that triggers all terminal processes as pathway activation crosses a single threshold [16]. Alternatively, individual terminal processes may be rescued one

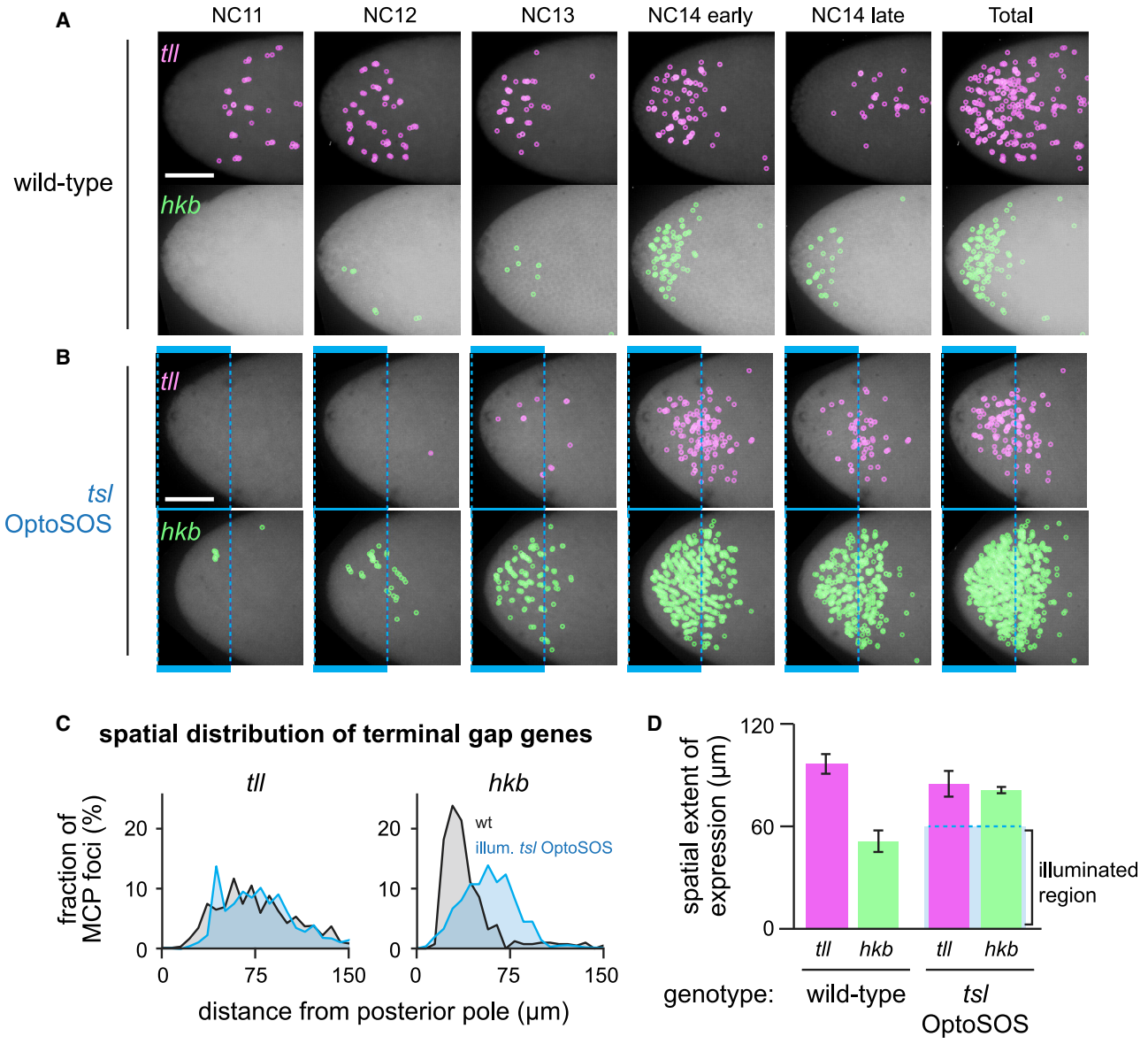

Figure 3. Light Stimulation Eliminates Spatiotemporal Differences in Terminal Gap Gene Expression

(A and B) Images are shown of OptoSOS embryos (in A) and OptoSOS-*tsl* embryos (in B) expressing MCP-mCherry and harboring MS2 stem loops driven by the *tll* or *hkb* upstream regulatory sequences (magenta and green, respectively). Embryos are oriented with posterior pole to the left. Images are maximum intensity projections across all z-frames and time points during the indicated nuclear cycles, with transcriptional foci marked with colored circles. In (B), 0.6-s pulses of saturating blue light were delivered every 30 s to the shaded region. Scale bar, 50 µm.

(C) Histogram showing the spatial distribution of transcriptional foci for *tll* (left panel) and *hkb* (right panel) for the endogenous gradient (embryos as in A; gray) and light stimulation (embryos as in B; blue). Each curve represents data pooled from at least three embryos.

(D) The spatial extent of gene expression for *tll* and *hkb* was measured for the endogenous pattern (left bars) and light stimulation (right bars) for the same embryos quantified in (C). Dotted blue box shows extent of illumination. Mean + SEM is shown for at least three embryos.

See also Figure S3, Table S2, and Video S2.

by one as the signaling input crosses distinct fate-specific thresholds [13]. To distinguish the number of cell-fate switches and identify their thresholds, we set out to map terminal phenotypes in response to variations in the strength optogenetic stimulus (Figure 4; see Table S1 for number of embryos with rescued phenotypes). Optogenetic control is also ideally poised to further distinguish what feature of an input signal is sensed—its level, duration above a threshold, or the total dose (i.e., intensity × time)—and we indicate which is varied in each experiment that follows.

We started with a brief light input—a single 5-min bolus of global, continuous illumination—reasoning that it would be much shorter than the 20- to 90-min periods of Erk activation that are typically triggered by RTK activation [31–34] and thus likely below the lower limit of detection by downstream phenotypic programs. Indeed, the 5-min pulse did not disrupt the development of a majority of

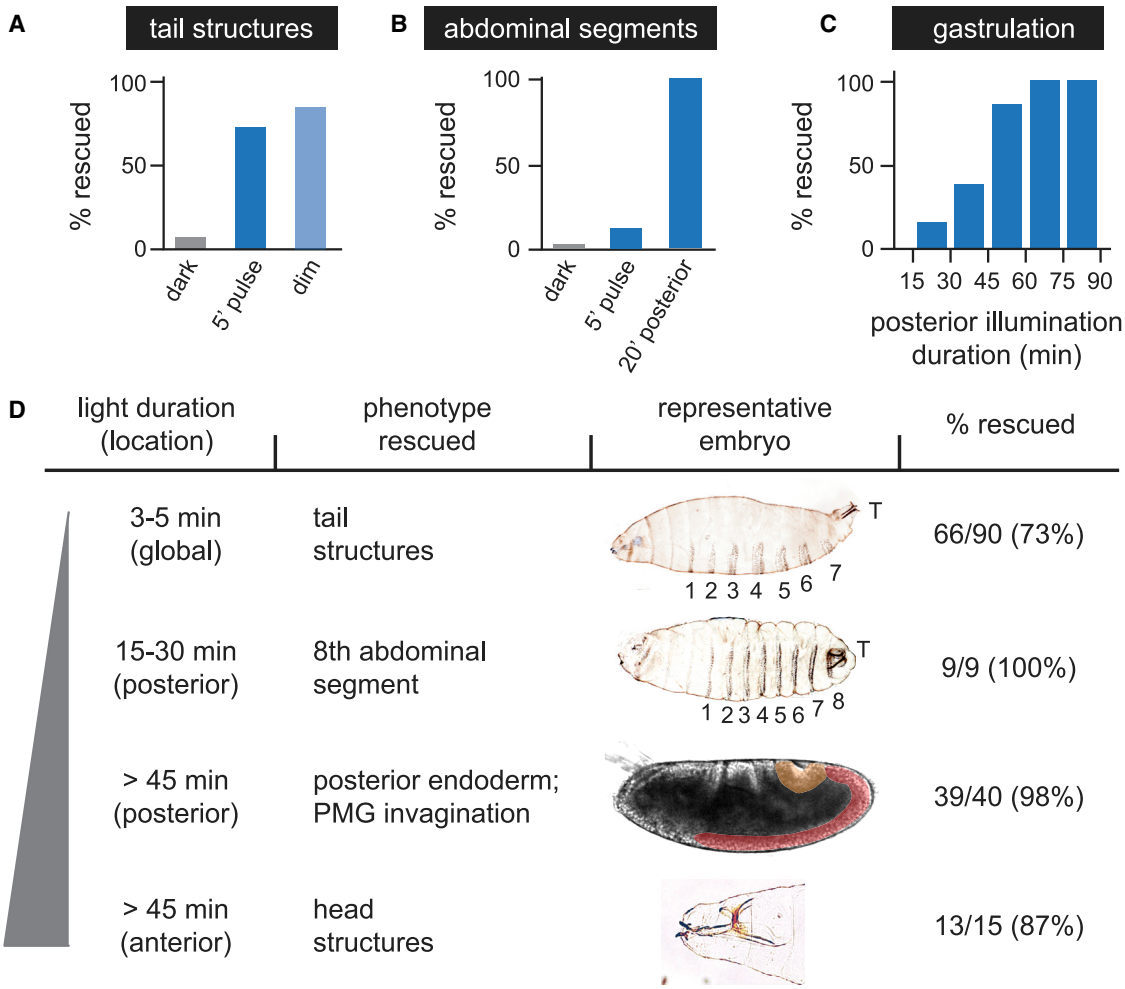

Figure 4. Three Durations of Terminal Signaling Trigger Distinct Developmental Programs

(A) The fraction of normal tail structures was quantified from embryos incubated in the dark, stimulated globally with a single 5-min bolus of saturating blue light ("5¢ pulse") or 1-s pulses of saturating blue light every 120 s ("dim"; see Figure S1B for quantification of Erk activity at similar light doses).

(B) The fraction of embryos with 8 abdominal segments was quantified from embryos incubated in the dark, subjected to a global 5-min bolus of saturating blue light (5¢ pulse) or illuminated for 20 min at the posterior-most 15% of the embryo with 0.6-s pulses of saturating blue light every 30 s.

(C) Posterior tissue movements during gastrulation were scored by differential interference contrast (DIC) imaging of embryos illuminated at the posterior pole.

(D) Developmental sequence of terminal phenotypes rescued in response to 0.6-s pulses of saturating blue light delivered every 30 s to the embryo's anterior-most 15% ("anterior") or posterior-most 15% ("posterior") or in response to 1-s pulses every 30 s delivered to the entirety of the embryo ("global"). The stimulus duration, spatial position, developmental phenotype, and a representative image are shown (OptoSOS-*trk* gastrulation and head structure images reproduced from Figures 2A and 2C). Embryos are oriented with anterior to the left and ventral downward.

See also Figure S4 and Tables S1 and S2.

OptoSOS embryos with wild-type terminal signaling, indicating that it was below the threshold for triggering substantial gain-of-function developmental defects (Figure S4A). However, we found that even this brief, uniform pulse of light was sufficient to restore tail structures in a majority of OptoSOS-*trk* embryos without altering other developmental programs (Figure 4A; Table S1). Tail structures were rescued even more efficiently by limiting the 5-min pulse to a narrower stimulation window of 90–150 min post-fertilization (Figures S4B and S4C), presumably corresponding to a period in which terminal gap gene expression can be triggered most efficiently (Figures 3A and 3B).

We next tested whether tail formation could also be driven by weaker inputs delivered over a longer time period and subjected embryos to 1-s pulses delivered every 120 s, a light intensity that results in less than 10% of the maximal Erk activity presented by the endogenous terminal gradient (Figure S2). Indeed, we found that equivalent rescue was obtained in response to either constant, low-intensity illumination or a brief, high-intensity pulse (Figure 4A). Together, these experiments reveal a set of remarkable requirements for a developmental cell fate choice: tail structure formation absolutely requires Ras/Erk signaling but is triggered at an extremely low total stimulus dose. Moreover, tail structures are rescued at the appropriate posterior position even by global illumination, a stimulus that does not contain any spatial information.

As we progressively increased the duration of illumination at the anterior or posterior pole, using 0.6-s pulses of saturating

blue light every 30 s, we observed that additional developmental processes were rescued in a well-defined sequence. The 8th abdominal segment was restored as the posterior light stimulus was increased to 20 min (Figure 4B), whereas normal gastrulation movements were only restored above 45 min of posterior illumination (Figure 4C). A similar 45-min pulse was also required at the anterior pole for the formation of head structures. We thus conclude that Ras/Erk activity is interpreted into at least three all-or-none developmental programs with duration thresholds spanning nearly an order of magnitude (5–45 min), at a stimulus intensity that drives comparable Erk phosphorylation to the endogenous maximum terminal level (Figure 4D; Table S1). Our data are strongly diagnostic of a multiple-threshold model of terminal signal interpretation: we find that increasing the total duration of light stimulation triggers distinct developmental processes in a well-defined order. Furthermore, in at least two cases, it appears that there is a correspondence between varying light intensity and duration, such that the phenotypic response would depend on the total dose of terminal signaling: tail formation (Figure 4A) and posterior midgut differentiation [13]. Importantly, the multiple-threshold model does not conflict with our prior observation of optogenetic rescue by a single, 45-min light stimulus. That is because mutant phenotypes appear to be restored in a cumulative fashion, so a given light stimulus rescues all developmental processes that are triggered at thresholds at or below this level.

Gastrulation Movements Are Robust to Variation in the Spatial Range of Terminal Patterning

The preceding experiments define the temporal requirements for terminal signaling, but what rules govern its permissible spatial parameters? We can again envision two extreme models. First, it is possible that only a highly restricted range of spatial pattern widths can support normal development, by balancing the proportion of cells committed to terminal and non-terminal fates. At the other extreme, many different spatial patterns could funnel into a proper developmental outcome [35], resembling the tolerance to variation in the bicoid morphogen gradient as gene dosage is varied [36] or the Shh gradient in the neural tube of $Gli3^{-/-}$ mice [37].

To test these possibilities, we varied the spatial domain of terminal signaling at our standard illumination intensity (0.6-s light pulses delivered every 30 s) and monitored a model developmental response: tissue morphogenesis during gastrulation. Terminal signaling at the posterior pole drives formation of posterior midgut (PMG), which invaginates and moves across the embryo's dorsal surface during germband elongation (GBE). GBE is thought to be driven both by a combination of "pushing" by cell intercalation at the ventral tissue (Figure 5A, red) and "pulling" by invagination of the posterior endoderm itself (Figure 5A, yellow) [38, 39]. Embryos derived from *trk* mutant mothers completely fail both PMG invagination and GBE, leading to buckling of the elongating tissue along the embryo's ventral surface [10] (Figure S5A). Consistent with this requirement, we found that PMG invagination and GBE were absent in dark-incubated embryos as well as over 90% of embryos that were illuminated only at the anterior pole (Figure S5B).

We proceeded to systematically vary the width of posterior pattern and measured both the perimeter of the PMG and the maximum extent of GBE, comparing each to wild-type embryos as controls. We found that the size of the posterior invagination scaled linearly in proportion to the illumination width (Figure 5B), with illumination regions up to 150 μm inducing the formation of posterior invaginations more than twice the maximum observed in wild-type embryos (Figure 5A, right). Yet despite the different proportion of terminal versus non-terminal tissue, the mechanical processes of gastrulation were broadly unaffected, with PMG invagination and germband elongation proceeding normally (Video S3). Quantitative analysis of the DIC videos indicated that germband elongation was indistinguishable from wild-type controls as the light pattern was varied over a 3-fold range, from 8% to 24% of the egg's length (Figures 5C and S5C). This result may partially explain the ease with which we obtained an optogenetic rescue even with imprecise illumination patterns. Furthermore, the ability to trigger morphogenetic movements at any spatial positions of interest will likely make OptoSOS-*trk* embryos a rich resource for informing and challenging models of tissue morphogenesis, along with other recent optogenetic tools for guiding tissue morphogenesis *in vivo* [40, 41].

DISCUSSION

Here, we demonstrate that a developmental signaling pattern can be erased and replaced with a synthetic, patterned stimulus. Our approach relies on the tools of cellular optogenetics: unlike pharmacological or genetic perturbations, light can be applied and removed quickly, focused with high spatial precision, or shaped into arbitrary spatial patterns. We found that a simple all-or-none blue light stimulus, delivered to the embryonic termini, is sufficient to convert a lethal loss-of-function phenotype to rescue the full *Drosophila* life cycle: embryogenesis; larval development; pupation; adulthood; and fecundity.

Our optogenetic rescue result provides two immediate insights into the interpretation of developmental RTK signaling. First, we find that recruiting the catalytic domain of SOS to the plasma membrane recapitulates all the essential developmental functions of Tor receptor tyrosine kinase signaling at the embryonic termini. This complete molecular sufficiency is non-obvious: we previously showed in mammalian cells that OptoSOS recruitment bypasses many intracellular pathways that are normally activated by RTKs (e.g., phosphatidylinositol 3-kinase [PI3K], Src, c-Jun N-terminal kinase [JNK], and glycogen synthase kinase 3 beta [GSK3β]) [17], some of which have been suggested to play roles in early *Drosophila* embryogenesis [42]. Nevertheless, our results are consistent with prior RNA sequencing (RNA-seq) data showing broad overlap between OptoSOS-stimulated and RTK-driven gene expression [22] and the observation that activating Ras pathway mutations are genetic suppressors of Tor partial loss-of-function alleles [43].

Second, our data suggest that the normally observed gradient of terminal signaling, resulting in spatially distinct domains of target gene expression, is not absolutely required for proper development. In support of this statement, our all-or-none rescue stimulus elicits a sharp boundary of OptoSOS membrane translocation [20], generates a steeper on-to-off switch in Erk activity than the endogenous terminal gradient (Figure S3), and

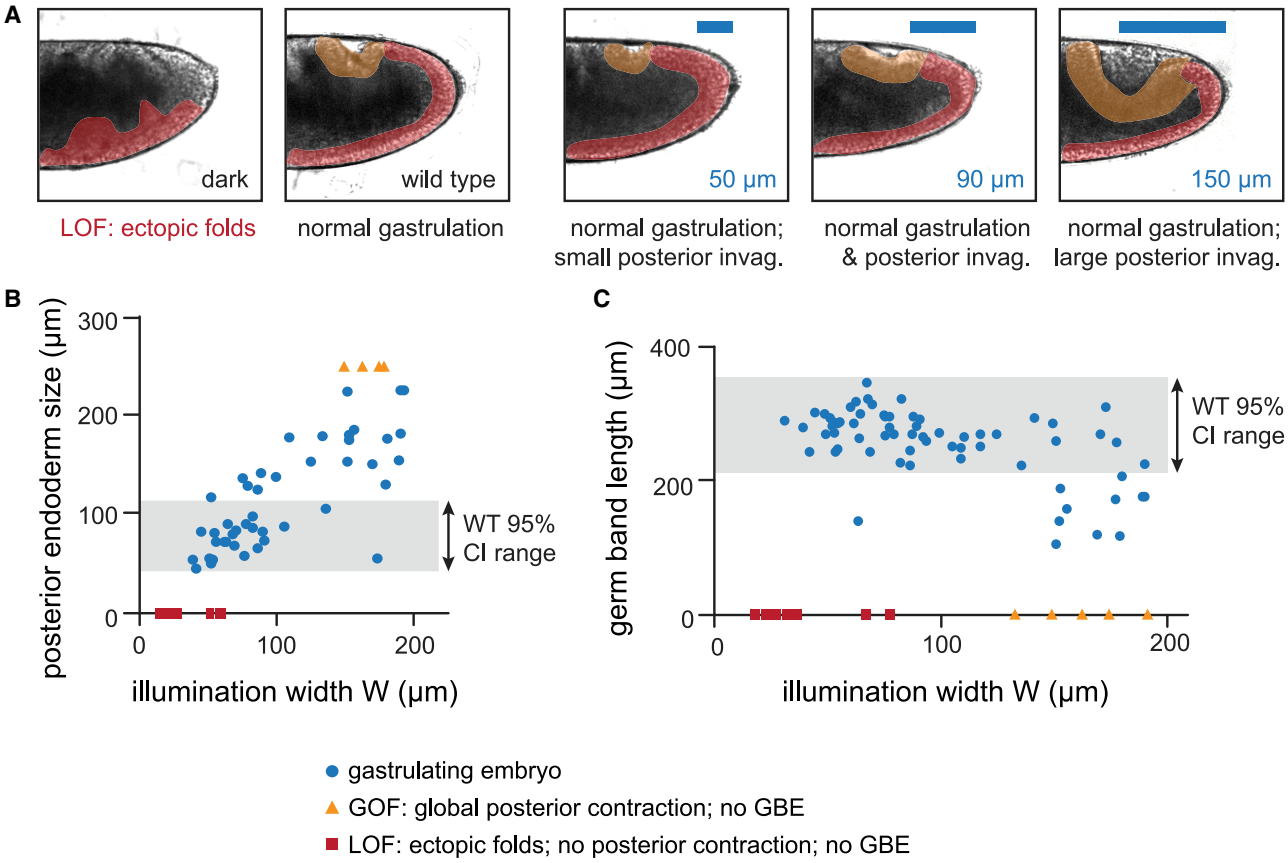

Figure 5. Tissue Morphogenesis Is Robust to Variations in Terminal Pattern Width

(A) Images of gastrulating wild-type embryos and OptoSOS-*trk* embryos stimulated with different illumination widths at the posterior pole with 90 min of 0.6-s pulses of saturating blue light delivered every 30 s. Yellow highlighted regions indicate posterior endoderm invagination, which expands as illumination width is increased. Red highlighted regions indicate the elongating germband tissue, which buckles in loss-of-function (LOF) embryos.

(B and C) Quantification of posterior endoderm perimeter (B) and germband elongation length (C) as a function of the illumination width from the posterior pole. For some embryos (yellow triangles), posterior contraction was so large as to completely disrupt germband elongation, a classic gain-of-function (GOF) phenotype. For others (red squares), no posterior contraction occurred, leading to LOF failure to extend a germband at all. For both (B) and (C), the shaded region indicates the normal wild-type size (mean ± 95% confidence interval), quantified from 27 wild-type embryos.

See also Figure S5, Table S2, and Video S3.

substantially reduces differences in the expression kinetics and spatial distribution for reporters of the terminal gap genes *tll* and *hkb* (Figure 3). The sufficiency of even coarse terminal patterns has been long suggested by classic experiments in which the Torso receptor or constitutively active Ras allele was injected at the termini of *tor* embryos, partially rescuing terminal processes [15, 16]; our data extend these early studies by quantifying the resulting patterns of gene expression and demonstrating the coarse input's sufficiency for complete phenotypic rescue. However, even though a simple all-or-none pattern is enough to rescue, our data do not indicate that terminal signaling functions as a single all-or-none switch. Instead, we find that distinct developmental events are triggered at vastly different durations of Erk signaling, from rescue of tail structures with as little as 5 min of stimulation to head structures and gastrulation movements only above 45 min. It is more likely that terminal processes operate as a series of switches with variable sensitivity, with stronger stimuli rescuing all phenotypes at or below that threshold.

How can such a simple stimulus pattern be reconciled with proper development? In wild-type embryos, terminal signaling triggers expression of the terminal gap genes Tll and Hkb in distinct domains, with Tll appearing earlier and extending further from the poles than Hkb [13]. Our optogenetic stimulus eliminates these differences, widening the expression domain of an *hkb* reporter to approximately match that of its *tll* counterpart. There is no reason to expect that this optogenetic scenario would prevent Tll and Hkb from playing their independent roles at the termini (e.g., Tll triggers posterior midgut invagination; Hkb represses Snail to block ventral furrow extension; Tll and Hkb each repress abdominal gap genes and specify endoderm cell fates) [28, 44–46]. Supporting this notion of robustness to the terminal signaling pattern, we previously found no decrease in embryo viability when light activation was added on top of the endogenous terminal pattern [20]; here, we further show that gastrulation movements are robust to variations in the spatial range of illumination (Figure 5). However, our data suggest that one important feature of the endogenous pattern would be entirely absent in light-rescued

embryos: a terminal domain with high levels of Tll but low levels of Hkb [47, 48]. How light-rescued embryos compensate for loss of this "Tll and not Hkb" signal, perhaps using other sources of anterior-posterior positional information, is an interesting question for future study [49]. This open question also reflects a broader challenge: we still lack a clear picture of the genetic circuits that decode developmental Erk signaling [50]. We expect that the approach we have taken here—combining controlled optogenetic stimulation with live-cell transcriptional imaging—could be applied to additional genes in the terminal response program to clearly define their signaling requirements in space and time.

It is also important to note that light-based rescue is far from perfect, with approximately 30% of embryos hatching after illumination. This loss in viability is likely to arise from both experimental and biological sources: challenges in reproducibly aligning embryos to the light pattern, leading to some error in the angle and extent of illumination at the termini; the procedure of mounting embryos in our imaging device for the entirety of embryogenesis; a loss of fitness from our simple all-or-none stimuli compared to the endogenous pattern; and the loss of parallel signaling pathways downstream of the Torso RTK that are bypassed by light-activated Ras. We anticipate that further advances in combining precise optical stimulation with non-invasive imaging will help to quantitatively determine how much each of these differences explains the increased lethality of our optogenetic stimulus relative to wild-type embryos.

There is considerable current interest in defining the rules that govern morphogenesis and patterning, both *in vivo* during embryo development and in engineered organoid-based systems. The optogenetic approaches defined here represent a first step toward the delivery of light-based programs to specific cells of interest within multicellular tissues. We find that even coarse synthetic signaling patterns can support normal tissue development and morphogenetic movements, suggesting that the tools of optogenetics and synthetic biology will likely be useful for generating developmental patterns that retain most or all of their essential functions [6, 51]. These capabilities could open the door to unprecedented control over developmental processes in both natural and synthetic multicellular systems.

STAR☆METHODS

Detailed methods are provided in the online version of this paper and include the following:

- KEY RESOURCES TABLE
- RESOURCE AVAILABILITY
  - Lead contact
  - Materials availability
  - Data and code availability
- EXPERIMENTAL MODEL AND SUBJECT DETAILS
  - *Drosophila melanogaster* stocks
  - Preliminary experiments to assess light-induced rescue of loss-of-function alleles
- METHOD DETAILS
  - Immunofluorescence quantification of Erk activity
  - Microscopy
  - Assessing and cuticle phenotypes
- QUANTIFICATION AND STATISTICAL ANALYSIS
  - Quantifying the spatial range of light-induced signaling
  - Quantifying the spatial range of gene expression
  - Assessing and quantifying gastrulation phenotypes

SUPPLEMENTAL INFORMATION

Supplemental Information can be found online at https://doi.org/10.1016/j.cub.2020.06.059.

ACKNOWLEDGMENTS

We thank Trudi Schüpbach and Yogesh Goyal for helpful discussions during the planning stages of our work, Romain Levayer for sharing the miniCic biosensor, Gerardo Jimenez for sharing DNA constructs used to design transcriptional reporters of *tll* and *hkb*, and Shannon Keenan for testing and characterization of the MS2 reporters lines. H.E.J. was supported by the NIH Ruth Kirschstein fellowship F32GM119297. This work was also supported by NIH grant DP2EB024247 and NSF CAREER Award 1750663 (to J.E.T.) and NIH grant 5R01HD085870 (to S.Y.S.). We also thank Dr. Gary Laevsky and the Molecular Biology Microscopy Core, which is a Nikon Center of Excellence, for microscopy support. Stocks obtained from the Bloomington Drosophila Stock Center (NIH P40OD018537) were used in this study.

AUTHOR CONTRIBUTIONS

H.E.J., S.Y.S., and J.E.T. conceived and designed the project and wrote the manuscript. N.J.V.D. designed and developed the *tll* and *hkb* MS2 fly strains. H.E.J. performed all experiments.

DECLARATION OF INTERESTS

The authors declare no competing interests.

Received: October 23, 2019
Revised: April 13, 2020
Accepted: June 17, 2020
Published: July 23, 2020

REFERENCES

1. Gurdon, J.B., and Bourillot, P.Y. (2001). Morphogen gradient interpretation. Nature *413*, 797–803.
2. Gregor, T., Tank, D.W., Wieschaus, E.F., and Bialek, W. (2007). Probing the limits to positional information. Cell *130*, 153–164.
3. Zagorski, M., Tabata, Y., Brandenberg, N., Lutolf, M.P., Tkačik, G., Bollenbach, T., Briscoe, J., and Kicheva, A. (2017). Decoding of position in the developing neural tube from antiparallel morphogen gradients. Science *356*, 1379–1383.
4. Coppey, M., Boettiger, A.N., Berezhkovskii, A.M., and Shvartsman, S.Y. (2008). Nuclear trapping shapes the terminal gradient in the Drosophila embryo. Curr. Biol. *18*, 915–919.
5. Johnson, H.E., and Toettcher, J.E. (2018). Illuminating developmental biology with cellular optogenetics. Curr. Opin. Biotechnol. *52*, 42–48.
6. Toda, S., Blauch, L.R., Tang, S.K.Y., Morsut, L., and Lim, W.A. (2018). Programming self-organizing multicellular structures with synthetic cell-cell signaling. Science *361*, 156–162.
7. Kriegman, S., Blackiston, D., Levin, M., and Bongard, J. (2020). A scalable pipeline for designing reconfigurable organisms. Proc. Natl. Acad. Sci. USA *117*, 1853–1859.
8. Goyal, Y., Schüpbach, T., and Shvartsman, S.Y. (2018). A quantitative model of developmental RTK signaling. Dev. Biol. *442*, 80–86.
9. Smits, C.M., and Shvartsman, S.Y. (2020). The design and logic of terminal patterning in Drosophila. Curr. Top. Dev. Biol. *137*, 193–217.

10. Schüpbach, T., and Wieschaus, E. (1986). Maternal-effect mutations altering the anterior-posterior pattern of the Drosophila embryo. Rouxs Arch. Dev. Biol. *195*, 302–317.
11. Klingler, M., Erdélyi, M., Szabad, J., and Nüsslein-Volhard, C. (1988). Function of torso in determining the terminal anlagen of the Drosophila embryo. Nature *335*, 275–277.
12. Casanova, J., and Struhl, G. (1989). Localized surface activity of torso, a receptor tyrosine kinase, specifies terminal body pattern in Drosophila. Genes Dev. *3* (12B), 2025–2038.
13. Greenwood, S., and Struhl, G. (1997). Different levels of Ras activity can specify distinct transcriptional and morphological consequences in early Drosophila embryos. Development *124*, 4879–4886.
14. Ghiglione, C., Perrimon, N., and Perkins, L.A. (1999). Quantitative variations in the level of MAPK activity control patterning of the embryonic termini in Drosophila. Dev. Biol. *205*, 181–193.
15. Lu, X., Chou, T.B., Williams, N.G., Roberts, T., and Perrimon, N. (1993). Control of cell fate determination by p21ras/Ras1, an essential component of torso signaling in Drosophila. Genes Dev. *7*, 621–632.
16. Sprenger, F., and Nüsslein-Volhard, C. (1992). Torso receptor activity is regulated by a diffusible ligand produced at the extracellular terminal regions of the Drosophila egg. Cell *71*, 987–1001.
17. Toettcher, J.E., Weiner, O.D., and Lim, W.A. (2013). Using optogenetics to interrogate the dynamic control of signal transmission by the Ras/Erk module. Cell *155*, 1422–1434.
18. Bugaj, L.J., Sabnis, A.J., Mitchell, A., Garbarino, J.E., Toettcher, J.E., Bivona, T.G., and Lim, W.A. (2018). Cancer mutations and targeted drugs can disrupt dynamic signal encoding by the Ras-Erk pathway. Science *361*, eaao3048.
19. Johnson, H.E., and Toettcher, J.E. (2019). Signaling dynamics control cell fate in the early Drosophila embryo. Dev. Cell *48*, 361–370.e3.
20. Johnson, H.E., Goyal, Y., Pannucci, N.L., Schüpbach, T., Shvartsman, S.Y., and Toettcher, J.E. (2017). The spatiotemporal limits of developmental Erk signaling. Dev. Cell *40*, 185–192.
21. Keenan, S.E., Blythe, S.A., Marmion, R.A., Djabrayan, N.J.-V., Wieschaus, E.F., and Shvartsman, S.Y. (2020). Rapid dynamics of signal-dependent transcriptional repression by Capicua. Dev. Cell *52*, 794–801.e4.
22. Wilson, M.Z., Ravindran, P.T., Lim, W.A., and Toettcher, J.E. (2017). Tracing information flow from Erk to target gene induction reveals mechanisms of dynamic and combinatorial control. Mol. Cell *67*, 757–769.e5.
23. Goglia, A.G., Wilson, M.Z., Jena, S.G., Silbert, J., Basta, L.P., Devenport, D., and Toettcher, J.E. (2020). A live-cell screen for altered Erk dynamics reveals principles of proliferative control. Cell Syst. *10*, 240–253.e6.
24. Grimm, O., Sanchez Zini, V., Kim, Y., Casanova, J., Shvartsman, S.Y., and Wieschaus, E. (2012). Torso RTK controls Capicua degradation by changing its subcellular localization. Development *139*, 3962–3968.
25. Moreno, E., Valon, L., Levillayer, F., and Levayer, R. (2019). Competition for space induces cell elimination through compaction-driven ERK downregulation. Curr. Biol. *29*, 23–34.e8.
26. Gillies, T.E., Pargett, M., Minguet, M., Davies, A.E., and Albeck, J.G. (2017). Linear integration of ERK activity predominates over persistence detection in Fra-1 regulation. Cell Syst. *5*, 549–563.e5.
27. Pignoni, F., Baldarelli, R.M., Steingrímsson, E., Diaz, R.J., Patapoutian, A., Merriam, J.R., and Lengyel, J.A. (1990). The Drosophila gene tailless is expressed at the embryonic termini and is a member of the steroid receptor superfamily. Cell *62*, 151–163.
28. Brönner, G., and Jäckle, H. (1991). Control and function of terminal gap gene activity in the posterior pole region of the Drosophila embryo. Mech. Dev. *35*, 205–211.
29. Santos, S.D., Wollman, R., Meyer, T., and Ferrell, J.E., Jr. (2012). Spatial positive feedback at the onset of mitosis. Cell *149*, 1500–1513.
30. Deneke, V.E., Puliafito, A., Krueger, D., Narla, A.V., De Simone, A., Primo, L., Vergassola, M., De Renzis, S., and Di Talia, S. (2019). Self-organized nuclear positioning synchronizes the cell cycle in *Drosophila* embryos. Cell *177*, 925–941.e17.
31. Marshall, C.J. (1995). Specificity of receptor tyrosine kinase signaling: transient versus sustained extracellular signal-regulated kinase activation. Cell *80*, 179–185.
32. Lim, B., Dsilva, C.J., Levario, T.J., Lu, H., Schüpbach, T., Kevrekidis, I.G., and Shvartsman, S.Y. (2015). Dynamics of inductive ERK signaling in the Drosophila embryo. Curr. Biol. *25*, 1784–1790.
33. Santos, S.D., Verveer, P.J., and Bastiaens, P.I. (2007). Growth factor-induced MAPK network topology shapes Erk response determining PC-12 cell fate. Nat. Cell Biol. *9*, 324–330.
34. Murphy, L.O., Smith, S., Chen, R.H., Fingar, D.C., and Blenis, J. (2002). Molecular interpretation of ERK signal duration by immediate early gene products. Nat. Cell Biol. *4*, 556–564.
35. Waddington, C.H. (1959). Canalization of development and genetic assimilation of acquired characters. Nature *183*, 1654–1655.
36. Driever, W., and Nüsslein-Volhard, C. (1988). The bicoid protein determines position in the Drosophila embryo in a concentration-dependent manner. Cell *54*, 95–104.
37. Balaskas, N., Ribeiro, A., Panovska, J., Dessaud, E., Sasai, N., Page, K.M., Briscoe, J., and Ribes, V. (2012). Gene regulatory logic for reading the Sonic Hedgehog signaling gradient in the vertebrate neural tube. Cell *148*, 273–284.
38. Irvine, K.D., and Wieschaus, E. (1994). Cell intercalation during Drosophila germband extension and its regulation by pair-rule segmentation genes. Development *120*, 827–841.
39. Collinet, C., Rauzi, M., Lenne, P.F., and Lecuit, T. (2015). Local and tissue-scale forces drive oriented junction growth during tissue extension. Nat. Cell Biol. *17*, 1247–1258.
40. Guglielmi, G., Barry, J.D., Huber, W., and De Renzis, S. (2015). An optogenetic method to modulate cell contractility during tissue morphogenesis. Dev. Cell *35*, 646–660.
41. Izquierdo, E., Quinkler, T., and De Renzis, S. (2018). Guided morphogenesis through optogenetic activation of Rho signalling during early Drosophila embryogenesis. Nat. Commun. *9*, 2366.
42. Pae, J., Cinalli, R.M., Marzio, A., Pagano, M., and Lehmann, R. (2017). GCL and CUL3 control the switch between cell lineages by mediating localized degradation of an RTK. Dev. Cell *42*, 130–142.e7.
43. Tsuda, L., Inoue, Y.H., Yoo, M.A., Mizuno, M., Hata, M., Lim, Y.M., Adachi-Yamada, T., Ryo, H., Masamune, Y., and Nishida, Y. (1993). A protein kinase similar to MAP kinase activator acts downstream of the raf kinase in Drosophila. Cell *72*, 407–414.
44. Reuter, R., and Leptin, M. (1994). Interacting functions of snail, twist and huckebein during the early development of germ layers in Drosophila. Development *120*, 1137–1150.
45. Weigel, D., Jürgens, G., Klingler, M., and Jäckle, H. (1990). Two gap genes mediate maternal terminal pattern information in Drosophila. Science *248*, 495–498.
46. Costa, M., Wilson, E.T., and Wieschaus, E. (1994). A putative cell signal encoded by the folded gastrulation gene coordinates cell shape changes during Drosophila gastrulation. Cell *76*, 1075–1089.
47. Kispert, A., Herrmann, B.G., Leptin, M., and Reuter, R. (1994). Homologs of the mouse Brachyury gene are involved in the specification of posterior terminal structures in Drosophila, Tribolium, and Locusta. Genes Dev. *8*, 2137–2150.
48. Singer, J.B., Harbecke, R., Kusch, T., Reuter, R., and Lengyel, J.A. (1996). Drosophila brachyenteron regulates gene activity and morphogenesis in the gut. Development *122*, 3707–3718.
49. Wu, L.H., and Lengyel, J.A. (1998). Role of caudal in hindgut specification and gastrulation suggests homology between Drosophila amnioproctodeal invagination and vertebrate blastopore. Development *125*, 2433–2442.
50. Patel, A.L., and Shvartsman, S.Y. (2018). Outstanding questions in developmental ERK signaling. Development *145*, dev143818.
51. Kicheva, A., and Rivron, N.C. (2017). Creating to understand - developmental biology meets engineering in Paris. Development *144*, 733–736.

52. Hunter, C., and Wieschaus, E. (2000). Regulated expression of nullo is required for the formation of distinct apical and basal adherens junctions in the Drosophila blastoderm. J. Cell Biol. *150*, 391–401.

53. Perkins, L.A., Holderbaum, L., Tao, R., Hu, Y., Sopko, R., McCall, K., Yang-Zhou, D., Flockhart, I., Binari, R., Shim, H.S., et al. (2015). The transgenic RNAi project at Harvard Medical School: resources and validation. Genetics *201*, 843–852.

54. Casanova, J., Furriols, M., McCormick, C.A., and Struhl, G. (1995). Similarities between trunk and spätzle, putative extracellular ligands specifying body pattern in Drosophila. Genes Dev. *9*, 2539–2544.

55. Savant-Bhonsale, S., and Montell, D.J. (1993). torso-like encodes the localized determinant of Drosophila terminal pattern formation. Genes Dev. *7* (12B), 2548–2555.

56. Fukaya, T., Lim, B., and Levine, M. (2016). Enhancer control of transcriptional bursting. Cell *166*, 358–368.

57. Ajuria, L., Nieva, C., Winkler, C., Kuo, D., Samper, N., Andreu, M.J., Helman, A., González-Crespo, S., Paroush, Z., Courey, A.J., and Jiménez, G. (2011). Capicua DNA-binding sites are general response elements for RTK signaling in Drosophila. Development *138*, 915–924.

58. Bothma, J.P., Garcia, H.G., Esposito, E., Schlissel, G., Gregor, T., and Levine, M. (2014). Dynamic regulation of eve stripe 2 expression reveals transcriptional bursts in living Drosophila embryos. Proc. Natl. Acad. Sci. USA *111*, 10598–10603.

59. Groth, A.C., Fish, M., Nusse, R., and Calos, M.P. (2004). Construction of transgenic Drosophila by using the site-specific integrase from phage phiC31. Genetics *166*, 1775–1782.

60. Bischof, J., Maeda, R.K., Hediger, M., Karch, F., and Basler, K. (2007). An optimized transgenesis system for Drosophila using germ-line-specific phiC31 integrases. Proc. Natl. Acad. Sci. USA *104*, 3312–3317.

61. Johnson, T.K., Moore, K.A., Whisstock, J.C., and Warr, C.G. (2017). Maternal torso-like coordinates tissue folding during *Drosophila* gastrulation. Genetics *206*, 1459–1468.

STAR☆METHODS

KEY RESOURCES TABLE

REAGENT or RESOURCE	SOURCE	IDENTIFIER
Experimental Models: Organisms/Strains		
D. melanogaster: UAS-optoSOS	[20]	N/A
D. melanogaster: 67;15	[52]	FBti0016179
D. melanogaster: mCherry-miniCic	[25]	N/A
D. melanogaster: mCherry-MCP	[21]	N/A
D. melanogaster: Hkb > MS2-Yellow	This paper	N/A
D. melanogaster: Tll > MS2-Yellow	[21]	N/A
D. melanogaster: TorRNAi	[53]	FBti0164703
D. melanogaster: *trk*^{1}	[10]	FBal0017039
Software and Algorithms		
Fiji		http://fiji.sc
MATLAB		https://www.mathworks.com

RESOURCE AVAILABILITY

Lead contact

Further information and requests for resources and reagents should be directed to and will be fulfilled by the Lead Contact, Jared Toettcher (toettcher@princeton.edu).

Materials availability

This study did not generate new reagents.

Data and code availability

All data and code is readily available upon request.

EXPERIMENTAL MODEL AND SUBJECT DETAILS

Drosophila melanogaster stocks

Transgenic UAS-optoSOS flies were produced as described previously [20] by fC31-based integration at either CH III 68A4 or CH II 25C6 and are driven maternally using P(mata-GAL-VP16)mat15 (67;15) for all experiments [52]. For rescue experiments the following LOF lines were used: *trk*^{1}, where a premature stop codon prevents production of a functional protein [10, 54]; Torso RNAi (P{TRiP.HMJ22419}attP40) [53]; and the *tsl*^{691} hypomorphic allele [55]. The *trk*^{1} and *tsl* lines were recombined with the optoSOS/67;15 lines to create the lines used for the rescues. The miniCic-OptoSOS embryos were generated by recombination with OptoSOS CH2 with miniCic [25] as well as 67;15 with miniCic, thus producing miniCic-optoSOS/miniCic-67;15/+ mothers.

For the MS2-MCP experiments, mCherry-MCP Ch III flies [56] were recombined with the OptoSOS-*trk* line. After crossing these flies with the 67 *trk*^{1}; 15 flies, virgin females were then crossed males harboring the corresponding MS2 construct. The tll-MS2 construct was produced as described in a recent paper [21]. Similarly, to generate the hkb-MS2 reporter, the hkb0.4 enhancer sequence was amplified from pCaSpeR-hs43-lacZ [57] via PCR. The resulting fragment was then inserted in the pBphi-evePromoter-24X MS2-yellow vector [58] via Gibson assembly. Transgenic lines carrying the hkb0.4-MS2 construct were generated by phiC31 integration in the 65B2 landing site (VK00033) [59, 60].

Preliminary experiments to assess light-induced rescue of loss-of-function alleles

We established embryos of three genotypes that each harbor our OptoSOS system and exhibit diminished or absent receptor-level activity: embryos produced by mothers that were homozygous for the *trk*^{1} amorphic allele or *tsl*^{691} hypomorphic allele, or embryos which carried an RNAi construct targeting Tor (see Drosophila melanogaster stocks section above). In each genetic background we monitored tissue movements during gastrulation to assess whether optogenetic stimulation could compensate for the loss of posterior terminal signaling (Figure S1). We chose this phenotype because posterior terminal signaling is required for invagination of the posterior midgut during gastrulation, and we previously found that illuminating OptoSOS embryos expands the domain of contractile midgut tissue across more than 80% of the embryo [19].

All three alleles failed to undergo posterior midgut invagination in the dark, indicative of strong loss-of-function of terminal signaling (Figure S1). We found that illuminating OptoSOS-*trk* and OptoSOS-Tor^{RNAi} embryos with 450 nm light produced tissue invagination during gastrulation, indicative of ectopic posterior midgut specification (Figure S1). No such tissue movements were observed in OptoSOS-*tsl* embryos (Figure S1), consistent with a recent report suggesting that Tsl plays an additional, terminal signaling-independent role in gastrulation [61]. Together, these experiments demonstrate that OptoSOS-*trk* and OptoSOS-Tor^{RNAi} embryos transition from a loss of terminal signaling in the dark to a strong gain-of-function phenotype upon illumination. Immunofluorescence staining for dpErk in OptoSOS-*trk* embryos (Figure 1A) revealed a complete loss of terminal Erk activity, consistent with prior reports [24]. To avoid any potential for incomplete knockdown or off-target effects by the Torso RNAi construct, we chose to focus on OptoSOS-*trk* embryos for all subsequent experiments.

METHOD DETAILS

Immunofluorescence quantification of Erk activity

For staining and quantification of doubly phosphorylated Erk (ppErk) (Figures 1A and S2), we collected images of embryos that had been fixed and stained after exposure to different pulse frequencies for ppErk (1:100; Cell Signaling). Activity was quantified similar to the method used for gene expression in [19] by tracing a contour around the edge of the embryo and normalized based on a co-stained histone-GFP control for each stimulation condition.

Microscopy

Cuticles were prepared for imaging as described previously [20] and imaged on Nikon Eclipse Ni through a 10X air objective using dark-field or brightfield microscopy. DIC and fluorescence imaging were performed on a Nikon Eclipse Ti spinning-disk confocal microscope. A 740-760nm band-pass filter (Chroma) was placed in the bright-field illumination light path to prevent unwanted optogenetic stimulation during imaging. Patterned optogenetic illumination was performed using a Mightex Polygon digital micromirror device (DMD) using an X-Cite XLED 450-nm blue LED. Spatial illumination of embryos was performed by drawing rectangular DMD patterns to stimulate the anterior pole, posterior pole, or both. The microscope's XY stage was then cycled between multiple embryos that were approximately aligned to these fixed patterns. Each embryo was stimulated with 600ms of DMD illumination every 30 s at an intensity of 4.5 mW/cm^2, leading to expected activity approximately equal to that of the maximal wild-type level (see Figure S2). Embryos were excluded from subsequent analysis if they were tilted more than 10 degrees from the illumination pattern, which was fixed to the horizontal axis.

Assessing and cuticle phenotypes

For cuticle counts, unfertilized or empty eggshells were excluded from all counts. Any visible filzkörper structures were marked as having "tail." Head structures with intact pharyngeal apparatus were marked as rescued. Abdominal segments were marked as rescued if the cuticle contained 8 intact denticle belts. Hatching rates are based on the number of empty eggshells versus the number of remaining embryos after 30+ hpf.

QUANTIFICATION AND STATISTICAL ANALYSIS

The number of embryos and replicates for each experiment (N values) are indicated in the figure legends and Table S2. For Figures S3G and S3H, the Student's t test was used to test for differences in the extent of Erk activation in wild-type versus light-stimulated embryos. The number of embryos is indicated on each figure panel.

Quantifying the spatial range of light-induced signaling

Successful optogenetic rescue requires that signaling be precisely patterned by local illumination. To verify that precise spatial patterns could be achieved, we set out to quantify the extent of SOS membrane translocation and Erk activity from a localized site of 450 nm light illumination and compared their spatial distributions to the endogenous gradient of Erk activity at the termini in nuclear cycle 14 (NC14) embryos. We made use of miniCic, a recently-developed fluorescent biosensor of Erk activity that is exported from the nucleus in response to phosphorylation by Erk (Figure S3A) [25].

For quantification of the spatial distribution of Erk activity in living OptoSOS-*trk* embryos, we illuminated individual miniCic-OptoSOS embryos with an all-or-none light pattern near the middle of the embryo and then collected a z stack of images in the OptoSOS and miniCic channels. We then computed maximum projections from these z stacks and plotted the intensity as a function of their distance from the illumination source. For quantifying the endogenous Erk gradient in a wild-type embryo, the maximum Erk activity and its decay as a function of distance was measured from the posterior pole. In both illuminated and endogenous Erk patterns, curves were normalized to their minimum and maximum values to obtain estimates of the percentage activity as a function of position in the embryo.

Imaging the termini of embryos expressing the miniCic biosensor (Figure S3B) revealed a graded decline in Erk activity from the poles similar to that obtained by phospho-Erk staining (Figure 1A). In contrast, we found that the intensity of both OptoSOS membrane translocation and miniCic activity dropped off sharply at the edge of the illuminated region (Figure S3B). Further quantification revealed that OptoSOS translocation and Erk activity returned to baseline levels within 60 μm from the edge of illumination versus

200 μm for the endogenous terminal gradient (Figure S3C). These results demonstrate that optogenetic stimulation can produce precise, localized patterns of Ras/Erk pathway activity at a fine scale relative to an endogenous pattern.

Quantifying the spatial range of gene expression

The range of terminal gene expression was assessed by processing the MCP-MS2 images in MATLAB (The MathWorks, Natick, Massachusetts). Burst were segmented from individual z-frames by applying a 6 μm^2 median filter and subtracting this from the original image. The resulting image is then binarized by thresholding. Bursts less than 3 pixels in size are removed before combining these pixels across all z frames. A mask of the embryo is created by k-means clustering of the starting image into two bins, followed by filling in of interior pixels and removal of stray pixels. This mask is then eroded by a 2 μm radius disk and bursts outside of this resulting mask are removed to prevent artifacts caused by debris on the surface of the embryo. There are no nuclei in this region, so it should not remove any actual bursts. Each remaining cluster of pixels is identified as a burst. The posterior edge of the embryo is determined from DIC imaging before each experiment. The distance the pattern extends from this edge is calculated in frames where there are at least three bursts. This is calculated by averaging this distance for the furthest three bursts from the pole. This is then averaged across the time course for each frame containing three or more bursts to calculate a final pattern width as in Figure 3D.

Assessing and quantifying gastrulation phenotypes

For experiments classifying gastrulation phenotypes by microscopy, germband elongation classification was performed based on the raw differential interference contrast (DIC) videos as follows:

Terminal loss-of-function-like: No posterior midgut invagination (PMG), the presence of ectopic folds during gastrulation. Complete absence of germband extension (GBE).

Normal: The posterior endoderm invaginates and travels along the dorsal surface toward the head. The final posterior-to-anterior length of posterior endoderm migration defines the 'GBE length' plotted in Figure 4C.

Terminal gain-of-function-like: Posterior invagination is abnormally large and does not migrate along the dorsal surface, so germband extension is lost.

The length of GBE was measured at the point which the germband stops constant forward progress toward the anterior pole. The perimeter of the PMG was measured as the largest contour after the initiation of the PMG invagination. Embryos which exhibited defects prior to NC14, were unfertilized, which were tilted relative to the illumination pattern greater than 10°, or where the parameter to be measured was not visible due to orientation of the embryo were excluded from counts. For Figures 4B and 4C, embryos which did not receive at least 60 minutes of light between the start of NC10 and 10 minutes before posterior gastrulation movements were also excluded from counts. For Figure 4C, embryos with illumination between 10%–30% of EL were included, No GBE ectopic phenotypes were excluded. Embryos were considered WT if found in the range of the 95% confidence interval for OreR controls. For experiments where light duration was varied, the duration included any illumination received prior to 10 minutes before the start of gastrulation.

Current Biology, Volume *30*

Supplemental Information

Optogenetic Rescue of a Patterning Mutant

Heath E. Johnson, Nareg J.V. Djabrayan, Stanislav Y. Shvartsman, and Jared E. Toettcher

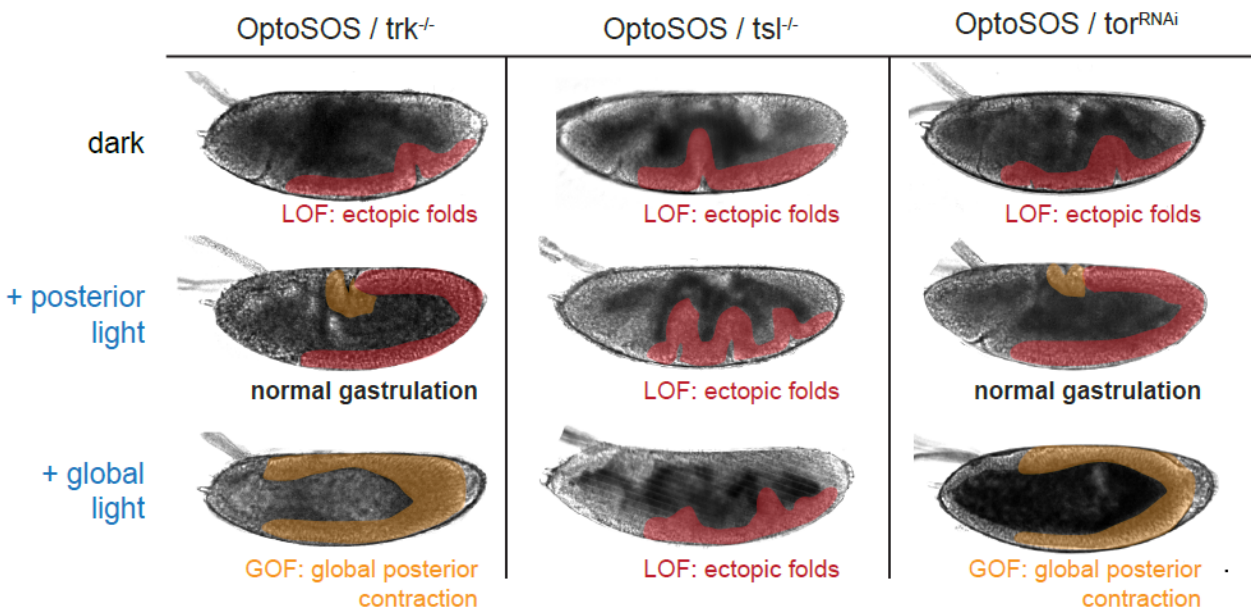

Figure S1: Characterizing optogenetic control in three Torso signaling pathway mutants. Related to Figure 1. Embryos were analyzed that expressed the OptoSOS system and were derived from mothers harboring loss-of-function Torso pathway alleles: homozygous *trk* (left), homozygous *tsl*, (middle) and 67;15>tor^{RNAi} (right). Each panel shows a representative embryo during gastrulation where the posterior midgut invagination (PMG invagination; yellow highlight) and elongating ventral mesoderm tissue (red highlight) are marked. Top row: all three mutants lead to loss-of-function phenotypes in the dark, including a failure to undergo PMG invagination and the appearance of ectopic folds along the embryo's ventral surface. Middle row: embryos were illuminated with a 0.6 sec of saturating 450 nm light every 30 sec, applied to the posterior-most 15% of the embryo. This stimulus rescues normal PMG invagination (yellow) and germ band elongation (red) in OptoSOS-*trk* and OptoSOS-tor^{RNAi} embryos. OptoSOS-*tsl* embryos still exhibit loss-of-function gastrulation phenotypes, including a lack of PMG invagination and ectopic folds. Bottom row: global illumination with 1 sec pulses of saturating 450 nm light every 30 sec leads to the large-scale formation of ectopic PMG and a massive contraction of the majority of the embryo in OptoSOS-*trk* and OptoSOS-tor^{RNAi} embryos but not in OptoSOS-*tsl* embryos. These data suggest that the *tsl* allele exhibits additional defects in tissue morphogenesis independently of its role in specifying terminal fates. All embryos in the figure are oriented with anterior to the left and ventral downward.

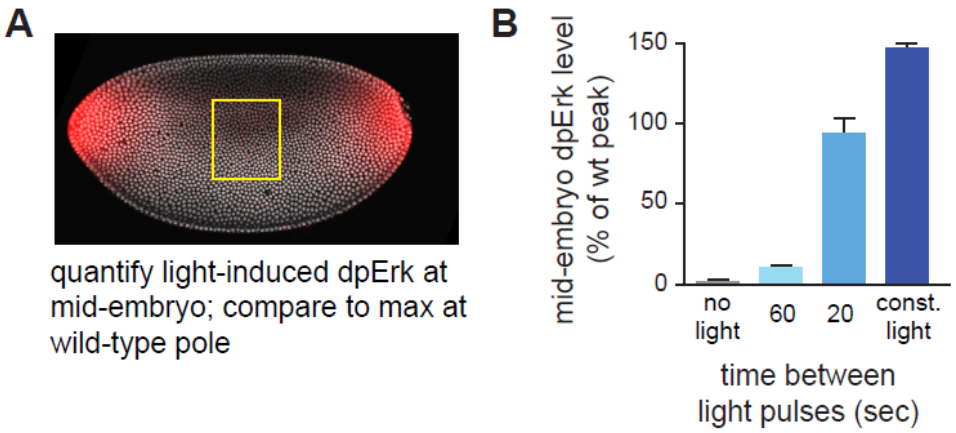

Figure S2: Titrating Erk phosphorylation using different light stimulus schedules. Related to Figure 2. (**A**) Nuclear cycle 12-14 OptoSOS embryos were illuminated for 1 hour under different stimulus conditions and then fixed and stained for doubly phosphorylated Erk (ppErk). The level of ppErk was quantified from a central embryonic region (yellow box) where endogenous terminal signaling would not contribute to Erk activity. As an internal standard, Erk phosphorylation was compared to the maximum level at the anterior pole of identically-stained wild-type embryos. A representative wild-type embryo exhibiting the normal terminal ppErk pattern is shown, reproduced from Figure 1A. Embryo is oriented with anterior to the left and ventral downward. (**B**) Quantification of ppErk levels in embryos stimulated with different cycles of saturating 450 nm light pulses: continuous light, a 1 sec pulse every 20 sec, a 1 sec pulse every 60 sec, or constant darkness. Illumination at 1 sec every 20 seconds led to ppErk levels comparable to the maximum level in the wild-type terminal pattern, whereas a 1 sec pulse every 60 sec drove steady-state ppErk levels at ~10% of the wild-type maximum. Error bars: standard deviation across spatial bins.

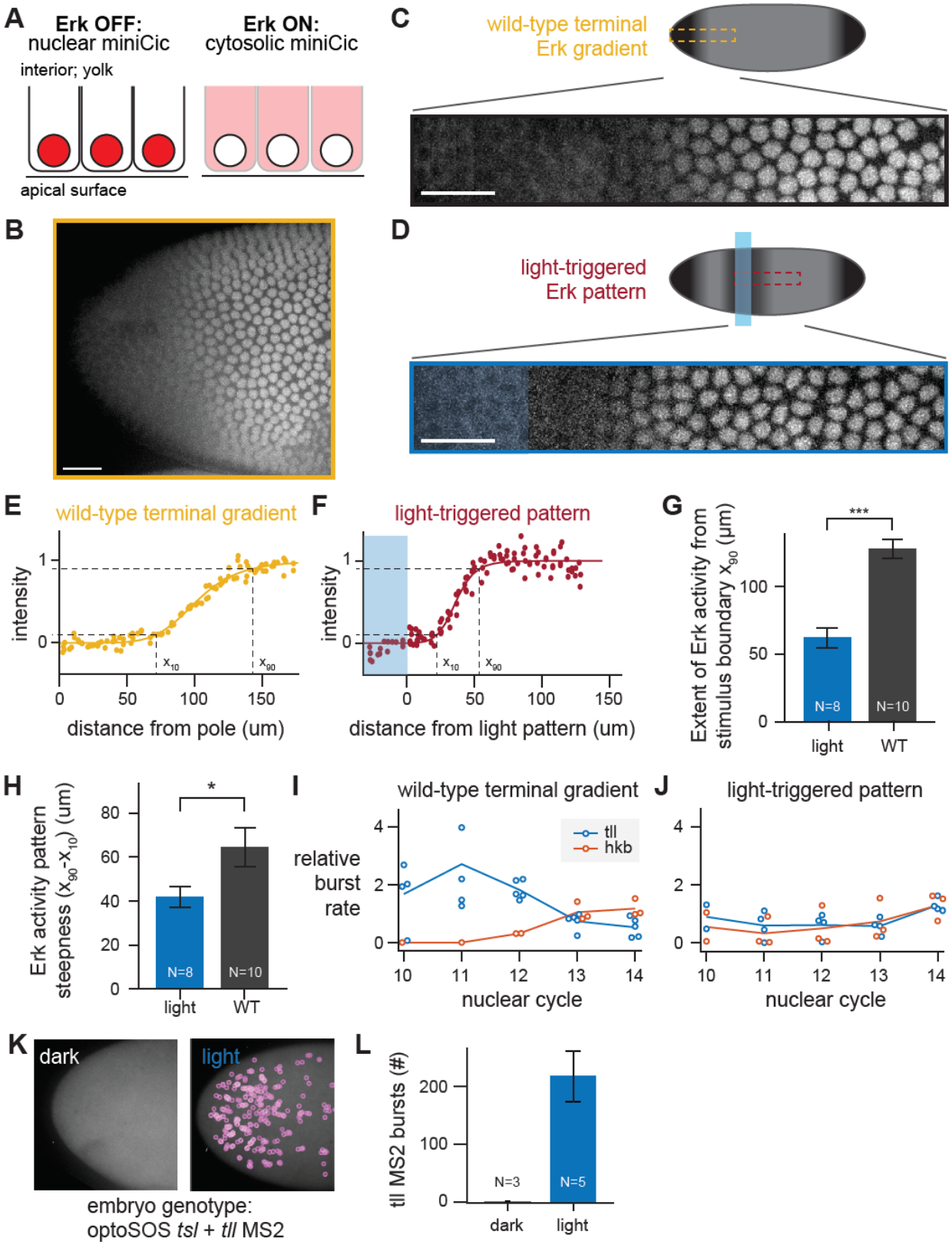
A
Erk OFF:
nuclear miniCic
Erk ON:
cytosolic miniCic
interior; yolk
apical surface
B
C
wild-type terminal
Erk gradient
D
light-triggered
Erk pattern
E
wild-type terminal gradient
intensity
distance from pole (um)
F
light-triggered pattern
intensity
distance from light pattern (um)
G
Extent of Erk activity from stimulus boundary x90 (µm)
***
N=8
N=10
light
WT
H
Erk activity pattern steepness (x90-x10) (um)
*
N=8
N=10
light
WT
I
wild-type terminal gradient
relative burst rate
tll
hkb
nuclear cycle
J
light-triggered pattern
nuclear cycle
K
dark
light
embryo genotype:
optoSOS tsl + tll MS2
L
tll MS2 bursts (#)
N=3
N=5
dark
light

Figure S3. Precise spatial patterning of Erk activity using light. Related to Figure 3. (**A**) A live-cell fluorescent biosensor of Erk activity (miniCic) was used to quantify the spatial distribution of Erk activity in living embryos. The miniCic biosensor is localized to the nucleus in the absence of Erk activity (left panel) and is phosphorylated and exported from the nucleus upon Erk activation (right panel). (**B**) Nuclear miniCic intensity imaged at the termini of wild-type nuclear cycle 14 (NC14) embryos, with a representative embryo shown oriented with its posterior pole to the left. A gradient of nuclear miniCic is formed, reflecting the endogenous gradient of Erk activity at the poles. Scale bar: 20 μm. (**C-D**) Comparison of the endogenous terminal pattern (in **C**) to an all-or-none light stimulus of 0.6 sec pulses of saturating 450 nm light delivered every 30 sec within the boxed region (in **D**). Representative miniCic fluorescence images from NC14 OptoSOS/miniCic embryos are shown, zoomed in from the indicated illumination regions (dashed boxes). Scale bars: 25 μm. (**E-F**) miniCic nuclear intensity was quantified from the embryo images in **C-D** as a function of position from the embryo pole (yellow curve) or the edge of the all-or-none light pattern (red curves). Best-fit Hill functions (solid lines) are shown. (**G-H**) Quantification of the length of gradient (in **G**) and gradient steepness (in **H**) for embryos stimulated as in **C**-**D**. '*' indicates $p < 0.05$ using Student's t test; '***' indicates $p < 0.01$ using Student's t test. The number of identically-stimulated embryos is shown for each bar. (**I-J**) Quantification of *tll* and *hkb* bursts over time for the embryos stimulated and analyzed in **Figure 3**. Points indicate the number of bursts per minute in each nuclear cycle, normalized to the average number of bursts across all nuclear cycles, for each embryo. Lines indicate the mean across multiple embryos; see **Table S2** for the number of embryos in each condition. (**K**) Still images OptoSOS-*tsl* embryos expressing MCP-mCherry and the *tll* upstream regulatory sequence driving MS2 stem-loops, incubated in the absence of 450 nm light or in response to an all-or-none light stimulus of 0.6 sec pulses of saturating 450 nm light delivered every 30 sec. Images are maximum intensity projected across all z-planes and time points. Representative embryos are oriented with posterior poles to the left. (**L**) Quantification of the number of transcriptional foci observed in embryos prepared as in **K**. The number of identically-stimulated embryos is shown for each bar.

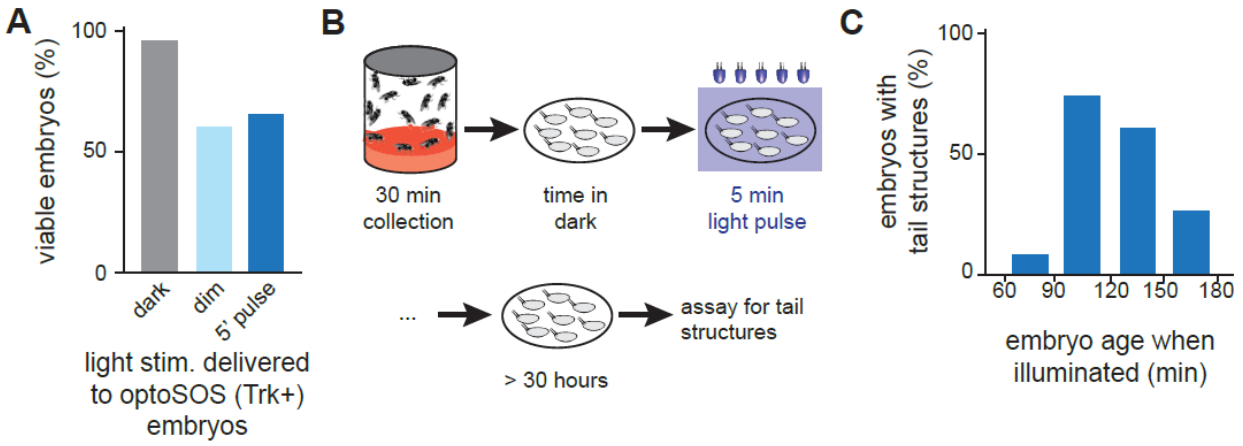

Figure S4: Programming of tail structures at low Erk levels. Related to Figure 4. (**A**) Assessing the effects of short-duration and low-intensity illumination on OptoSOS embryos that still exhibit normal endogenous terminal signaling. Embryos were incubated in the dark, stimulated globally with a 1 sec light pulse delivered every 120 sec ("dim"), or incubated under a single 5 min bolus of constant, saturating 450 nm light ("5' pulse"), and viability was assessed. Under these conditions, a majority of larvae still hatch and appear normal, indicating that the light intensity used to rescue tail structures is below the threshold for eliciting strong gain-of-function phenotypes. "Dim" light indicates 1 sec pulses of saturating 450 nm light every 120 sec, expected to lead to Erk activity less than 10% of maximal levels (see **Figure S2**). (**B**) Schematic of experiment to define the time window during which tail structures are specified. OptoSOS-*trk* embryos were collected over a 30 min period, incubated in the dark for varying amounts of time, and then globally illuminated with a 5 min light pulse. Cuticle preparations were then used to assess the formation of tail structures at the end of embryogenesis. (**C**) The fraction of embryos with normal tail structures was defined in each 30 min collection window, with most embryos harboring tails when stimulated in a 1 h window, 90-150 min after fertilization.

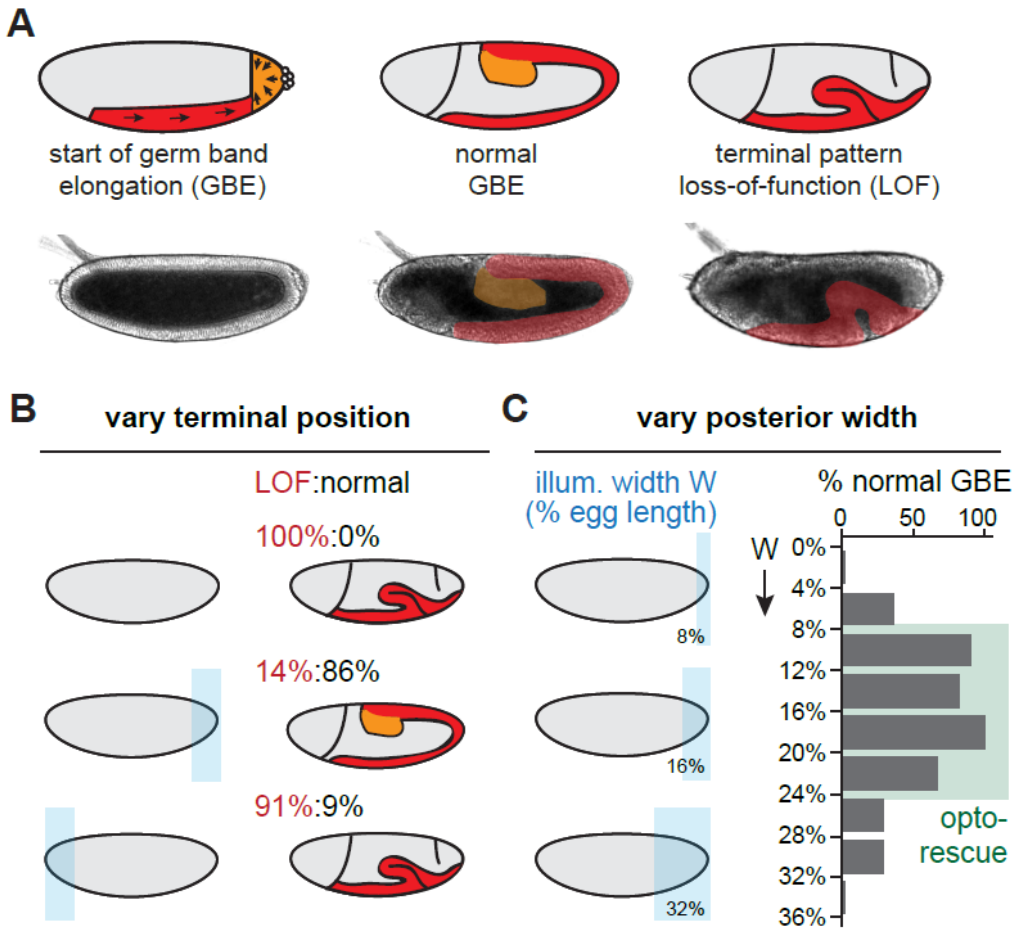

Figure S5. The lower limit of spatial signaling required for tissue morphogenesis. Related to Figure 5. (**A**) Schematic of posterior tissue movements during germ band elongation (GBE), with representative images for each phenotype shown below. Left: During germ band elongation, cells migrate to the ventral surface (red highlight) and intercalate, while the posterior endoderm (orange highlight) constricts and internalizes. Middle: This results in the large-scale movement of posterior tissue along the dorsal surface towards the head. Right: In the absence of terminal signaling, germ band elongation is blocked, leading to buckling of ventral tissue. All embryos are oriented with anterior to the left and ventral downward. (**B-C**) Optogenetic dissection of the spatial requirements for terminal signaling in gastrulation. All embryos were stimulated with a 90 min overall stimulus of 0.6 sec pulses of saturating 450 nm light delivered every 30 sec to the indicated spatial regions. "Normal" gastrulation was defined as successful posterior invagination and a germ band whose length was within the 95% confidence interval obtained from 27 wild-type embryos. A loss-of-function ("LOF") embryo was defined by a lack of posterior invagination and germ band elongation. (**B**) Gastrulation was scored for embryos that were kept in the dark or illuminated at either the anterior or posterior pole and monitored by differential interference contrast (DIC) imaging. (**C**) Gastrulation was scored for embryos that were illuminated with different posterior pattern widths, from 0-36% of the embryo's length. Illumination widths that produce normal gastrulation in a majority of embryos are marked with a green box. For **B-C**, normal gastrulation is defined by presence of posterior invagination and a germ band that extends to a length within the wild-type 95% confidence interval.

stimulus duration	tail structures	proper segmentation	gastrulation movements	head structures	hatching
dark	33/204 (16%)	3/109 (2.7%)	0/10 (0%)	0/5 (0%)	0/200 (0%)
5 min	**G: 66/90 (73%)**	P: 21/172 (12.2%)	ND	ND	ND
15-30 min	**P: 9/9 (100%)**	**P: 9/9 (100%)**	P: 4/69 (5.7%)	A: 0/8 (0%)	ND
45-90 min	**7/7 (100%)**	**6/7 (86%)**	**P: 39/40 (97.5%)**	**A: 13/15 (87%)**	**9/31 (29%)**

Table S1: Quantification of embryo phenotypes from optogenetic experiments and dark-incubated controls. Related to Figures 2 and 4. Each entry represents the total number of embryos whose structures could be assessed under light stimulation of the duration indicated. In each entry case, the location of illumination is noted (P = posterior; A = anterior; G = global). All anterior and posterior light stimuli consisted of 0.6 sec pulses of saturating 450 nm light delivered every 30 sec; global illumination was delivered using 1 sec pulses of saturating 450 nm light every 30 sec. Red entries indicate a failure to rescue (normal phenotype less than 20%), whereas green bolded entries indicate successful rescue. Data is taken from multiple experiments described in Figure 2 and Figure 4.

Figure	# of embryos per condition
2A	15
2B	7
2C	22
2D	31, 200
3C,D	6, 3, 5, 5
4A	204, 90, 68
4B	109, 172, 9
4C	8, 43, 26, 7, 4, 30
5B	70 (WT = 27)
5C	82 (WT = 27)
S2B	52, 28, 26, 10
S3G,H	8, 10
S3I,J	6, 3, 5, 5
S3L	3, 5
S4A	88, 21, 117
S4C	102, 90, 81, 139
S5B	10, 44, 34
S5C	2, 11, 20, 17, 4, 3, 7, 7, 3 (WT = 27)

Table S2: Number of embryos quantified in each experiment. Related to Figures 2-5 and S2-S5. Comma-separated numbers indicate the number of embryos quantified in each experimental condition, from left to right as indicated in the corresponding figure.